Advances in Nano Research, *Vol. 1, No. 4 (2013) 219-228*
DOI: http://dx.doi.org/10.12989/anr.2013.1.4.219

On the preparation of iron pyrite from synthetic and natural targets by pulsed electron deposition

Omar Al-Shareeda[1], Redhouane Henda*[1], Allan Pratt[2] and Andrew M. McDonald[3]

[1]*School of Engineering, Laurentian University, Sudbury, P3E 2C6, Canada*
[2]*CANMET Mining and Mineral Sciences Laboratories, Natural Resources Ottawa, K1A 0G1, Canada*
[3]*Earth Science Dept., Laurentian University, Sudbury, P3E 2C6, Canada*

(Received March 7, 2013, Revised July 12, 2013, Accepted November 6, 2013)

Abstract. We report on the preparation of iron pyrite (FeS_2) using pulsed electron ablation of two targets, namely, a mixture of sulfur and iron compound target, and a natural iron pyrite target. Thin films of around 50 nm in thickness have been deposited on glass substrates under Argon background gas at 3 mTorr, and at a substrate temperature of up to 450℃. The thin films have been analyzed chemically and examined structurally using x-ray diffraction (XRD), x-ray photoelectron spectroscopy (XPS), and visible Raman spectroscopy. The morphology and thickness of the films have been assessed using scanning electron microscopy (SEM) and visible spectroscopic reflectance. The preliminary findings, using a synthetic target, show the presence of iron pyrite with increasing proportion as substrate temperature is increased from 150℃ to 250℃. The data have not shown any evidence of pyrite in the deposited films from a natural target.

Keywords: iron pyrite; pulsed electron beam ablation; thin films; photovoltaics

1. Introduction

The mineral iron pyrite is a widely available metal sulfide and a source for obtaining pure iron. It crystallizes in a cubic cell with 12 atoms/cell and belongs to the space group symmetry T_h^6 (Slater 1965). Pyrite has a set of very interesting properties. With a very high absorption coefficient (6×10^5 cm^{-1} at 2 eV), appropriate energy band gap (0.95 eV) (Schlegel and Wachter 1976) and consisting of abundant, inexpensive and non-toxic elements, iron pyrite has received much interest as a material for thin film solar cells (Jaegermann and Tributsch 1983, Ennaoui and Tributsch 1984, Wadia *et al*. 2009). In a recent study, Wadia *et al*. (2009) have evaluated over 20 promising semiconducting materials and found out that a dozen are abundant enough to meet or exceed annual worldwide energy demand. Among these, nine have a significant raw material cost reduction over traditional crystalline silicon, the most commonly used light-absorbing material in mass production today. They have shown that iron pyrite is several orders of magnitude better than any alternative material in terms of both cost (cents/watt) and abundance. Although pyrite has a smaller band gap than silicon (1.1 eV), its high natural abundance translates to an estimated 0.000002 ¢/W material extraction cost, assuming an annual output of approximately 10^{10} TWh

*Corresponding author, Professor, E-mail: rhenda@laurentian.ca

http://www.techno-press.com/?journal=anr&subpage=7 ISSN: 2287-237X (Print), 2287-2388 (Online)

(Wadia *et al*. 2009). The modest efficiency losses of unconventional solar cell materials would be offset by the potential for scaling up while saving significantly on materials costs. Since pyrite is so inexpensive, only 4% efficiency is needed to be competitive with current-generation 20%-efficient absorbers.

Over the past three decades, concerted research efforts have been devoted to the preparation of iron pyrite in thin film form as a potential low-cost absorber for next generation photovoltaic devices. Various techniques have been used to synthesize pyrite films, including chemical vapor deposition, molecular beam epitaxy, pulsed laser deposition, sulfurization of iron or iron oxide, spray pyrolysis and thermal evaporation, and magnetron sputtering (Jaegermann and Tributsch 1983, Seehra *et al*. 1979, Yokoyama *et al*. 2006, Nakamura and Yamamoto 2001, Bronolda *et al*. 1997, Rezig *et al*. 1992, Willeke *et al*. 1992, Chatzittheodorou *et al*. 1986). While most of the preparation methods consist of multiple steps, e.g., sulfurization in sulfur-rich atmosphere or deposition from compositionally different targets, pyrite deposition from a single target has proven to be quite elusive. Pyrite has no melting point but exhibits a peritectic decomposition point at 1016 K where it decomposes to troilite (FeS) and sulfur. On the other hand, the vapor pressure of sulfur is much smaller than the vapor pressure of iron (Lupis 1983). For these reasons, melt growth techniques are not best suited for the growth of films of pure iron pyrite from a single target, and more advanced deposition techniques need to be evaluated in order to understand the challenges encountered in iron pyrite thin film deposition.

In this paper, we report on our attempt toward the preparation of pyrite from a single compound target (synthetic; natural) using the technique of pulsed electron deposition (PED). To the best of our knowledge no such work has been reported yet using PED, and hence the motivation for this work. The results from the various analytical measurements on the deposited films are examined and discussed.

2. Experimental procedure

The thin films were deposited in a channel-spark pulsed electron beam ablation system, PEBS-20 model with a pulse duration of 100 ns (Neocera, Inc., USA). The pulsed electron beam source consists of a trigger, a hollow cathode, and a dielectric capillary tube. A snapshot of a typical deposition run is illustrated in Fig. 1, where the tip of the dielectric tube close to the target and the vertically expanding plasma towards the substrate can be seen. A two-inch diameter and ¼ inch-thick disc consisting of a mixture of elemental iron and sulfur (purity 99.9%, SuperConductor Materials Inc., USA) was used as the target material. The natural target is a 1-inch diameter and 0.25-inch thick disk of pyrite from Logrono mine in Spain (Bestcrystals, USA). The glass substrates, namely, corning and pyrex (Vin Karola Instr., USA), were cut into pieces of ½ × ½ inch^2. The substrate was sonically cleaned at 50^{o}C prior to deposition. The substrate was further rinsed with acetone followed with methanol, while the target was cleaned in acetone. The electron charging voltage was set to 15 kV with a fixed pulse frequency of 5 Hz. A constant number of 3000 electron pulses was used throughout the experiments. Prior to film deposition experiments, the deposition chamber was evacuated to 2.5×10^{-5} Pa before admitting the background gas into the chamber at a pressure of 3 mTorr. The distance between the target and electron gun alumina tube tip was kept at ~3 mm whereas the target to substrate distance was kept at 50 mm. Prior to deposition, the target was pre-ablated by the electron beam over 3000 pulses at 1 Hz and 10 kV. In order to evaluate the effect of temperature on pyrite formation, the substrate temperature was varied

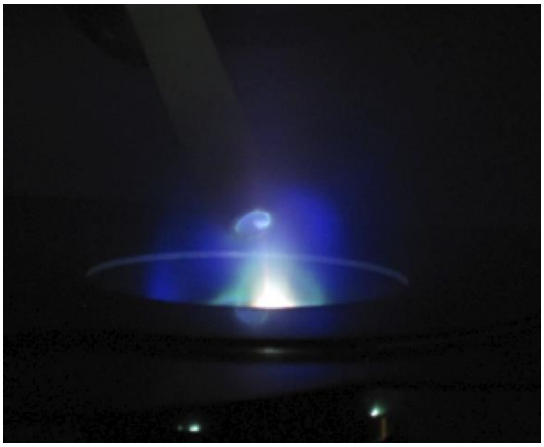

Fig. 1 Snapshot of a typical experimental run

between room temperature (RT) and 250℃ (for synthetic target) and between RT and 450℃ (for natural target).

Subsequently, the deposited films were characterized using XPS, XRD and Raman spectroscopy. XPS spectra were collected using a Kratos Axis Ultra X-ray photoelectron spectrometer. The system can probe the surface of the sample to a depth of 7-10 nm, and has detection limits ranging from 0.1 to 0.5 atomic percent depending on the element. Survey scan analyses were carried out with an analysis area of 300 µm x 700 µm and a pass energy of 160 eV. XRD patterns were obtained using a Rigaku D/MAX 2500 rotating anode powder diffractometer using monochromatic CuKα radiation. The XRD system was operated under the following conditions: a fixed grazing angle of 0.5º in the two-theta angular range 20º- 70º, step size = 0.020º, scan speed = 1º/min, voltage = 50 kV, and current = 260 mA. Phase identification was achieved using JADE version 9.0 coupled with the ICSD and ICDD diffraction databases. Raman data were collected in backscattered mode with a HORIBA Jobin Yvon XploRA spectrometer interfaced with an Olympus BX 41 microscope (100*x* magnification, estimated spot size of 2 μm), a 1200 grating and an incident laser excitation radiation wavelength of 532 nm. Raman spectra (average of ten, 10 s spectra) were obtained between 50 cm^{-1} and 1100 cm^{-1}. Calibration was made using the 521 cm^{-1} line of a silicon wafer. The deposited films thickness and morphology were evaluated using SEM and visible reflection spectroscopy. SEM Field Emission measurements were made on a JEOL 6300 operated at 20 kV. The samples were carbon coated prior to examination. Film thickness was obtained with M-Probe series reflectometer (Semiconfsoft, USA), where experimental data were fitted by means of a modified Marquardt–Levenberg minimization built in the accompanying software.

3. Results and discussion

3.1 Synthetic target

X-ray diffraction pattern of the synthetic target material is shown in Fig. 2, where the positions of iron and sulfur lines are indicated beneath the pattern. No peaks corresponding to pyrite could

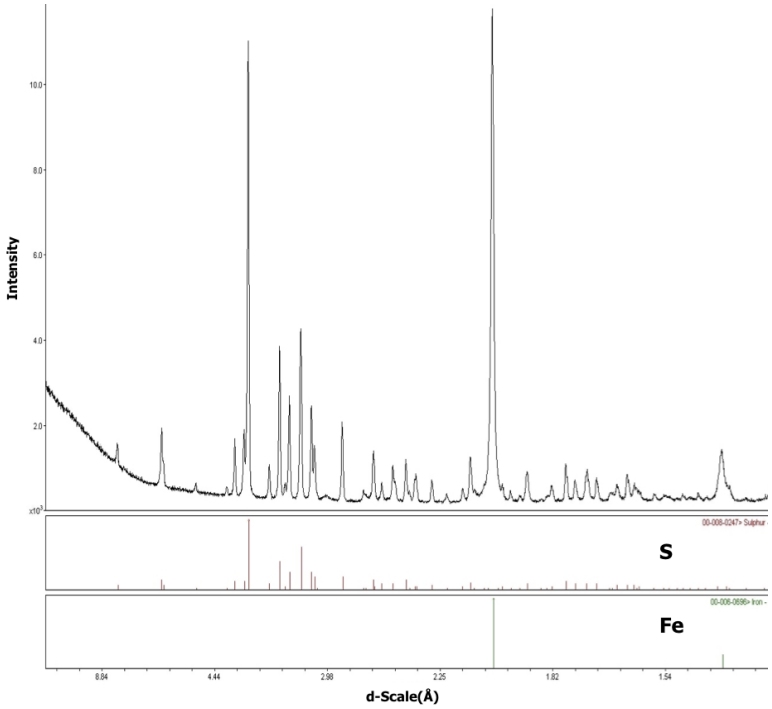

Fig. 2 XRD pattern of the synthetic target material

be detected, which indicates that the target material is a mere mixture of elemental iron and sulfur, contrary to the claim of the target supplier.

XRD patterns of the deposited films at different substrate (only data for corning are shown) temperatures are reported in Fig. 3. As can be seen, only two peaks are well resolved relatively to the background noise for both substrates (films on pyrex show peaks at same positions as well) especially at high substrate temperature. The peak around a 2θ of 41° corresponds to plane (211) in pyrite (Rezig *et al*. 1992, Shembel *et al*. 2006), while the second peak around 36° could not be attributed to pyrite but could rather correspond to either FeO or troilite. It is to be noted here that only at very low grazing angles (0.5° in this case) could XRD yield relatively resolved peaks – for instance, at a grazing angle of 5° only a background noise is obtained. Accordingly, XRD findings are inconclusive. Fig. 4 shows XPS spectra of the films on corning and pyrex at a substrate temperature of 250℃. The sulfur 2*p* results, viz., Fig. 4(a) and 4(c), at ~162.3 eV ($2p_{3/2}$) is an indication of the presence of pyrite in the films (Wagner *et al*. 1979, van der Heide *et al*. 1980). The iron 2*p* signal, viz., Fig. 4(b) and 4(d), at ~707 eV is characteristic of pyrite (Wagner *et al*. 1979, van der Heide *et al*. 1980).

In addition to pyrite, XPS measurements have revealed the presence of troilite in about equal proportion to pyrite but decreasing with increasing substrate temperature. Other detected phases correspond to iron oxides/oxyhydroxides and elemental sulfur/sulfur oxides in decreasing abundance, respectively. Since XPS is a predominately surface characterization method, the various oxide compounds are not necessarily present in the 'bulk' of the deposited films but rather most likely are only to be found at the surface and within a few nanometers beneath the surface of the films.

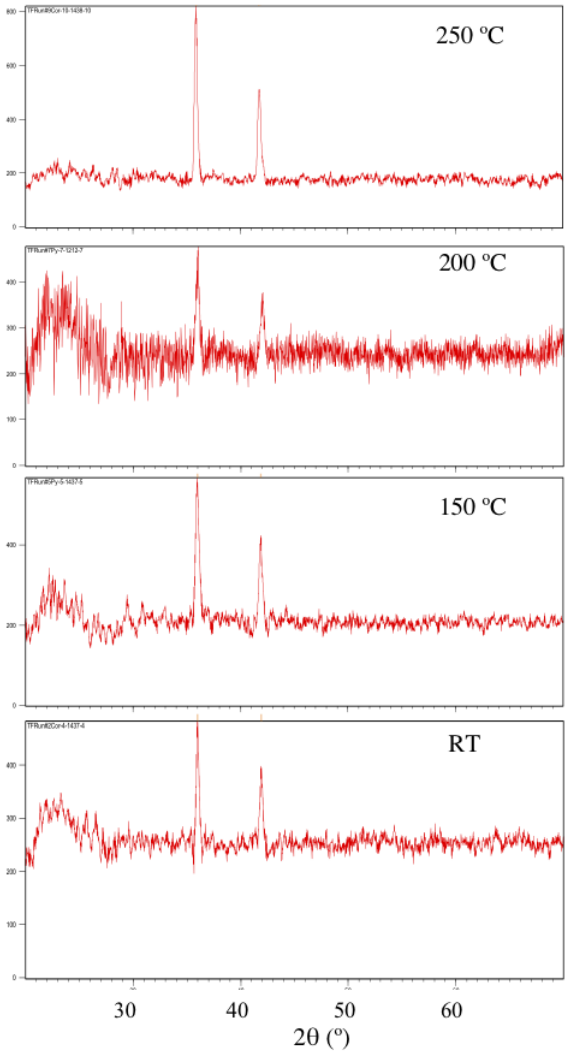

Fig. 3 XRD patterns of films on corning at different substrate temperatures

The deposited films have also been analyzed using Raman spectroscopy. The Raman spectrum of the deposited films is shown in Fig. 5. It has two typical peaks, at around 336 cm^{-1} and 371 cm^{-1}, which are attributed to pyrite. The difference, i.e., 35 cm^{-1} (Fig. 5), between the two peaks in the films corresponds to the same difference between the peaks (379 cm^{-1} and 344 cm^{-1}) in the Raman band of pure iron pyrite, as shown in Fig. 6. The two other peaks at ~463 cm^{-1} and 823 cm^{-1} in the Raman band of the deposited films are attributed to corning (Sasaki 1997, Kim 1998), although the peak at 463 cm^{-1} is also typical of polymeric sulfur (Parker and Hope 2010).

A typical transversal morphology of the films is shown in Fig. 7. A visual inspection of the film shows a rugged surface consisting of nano-sized particulates. The thickness of the film varies from about 50 nm to 100 nm in good accordance with visible reflectance spectroscopy measurements (not shown here), which yield a value of ~50 nm.

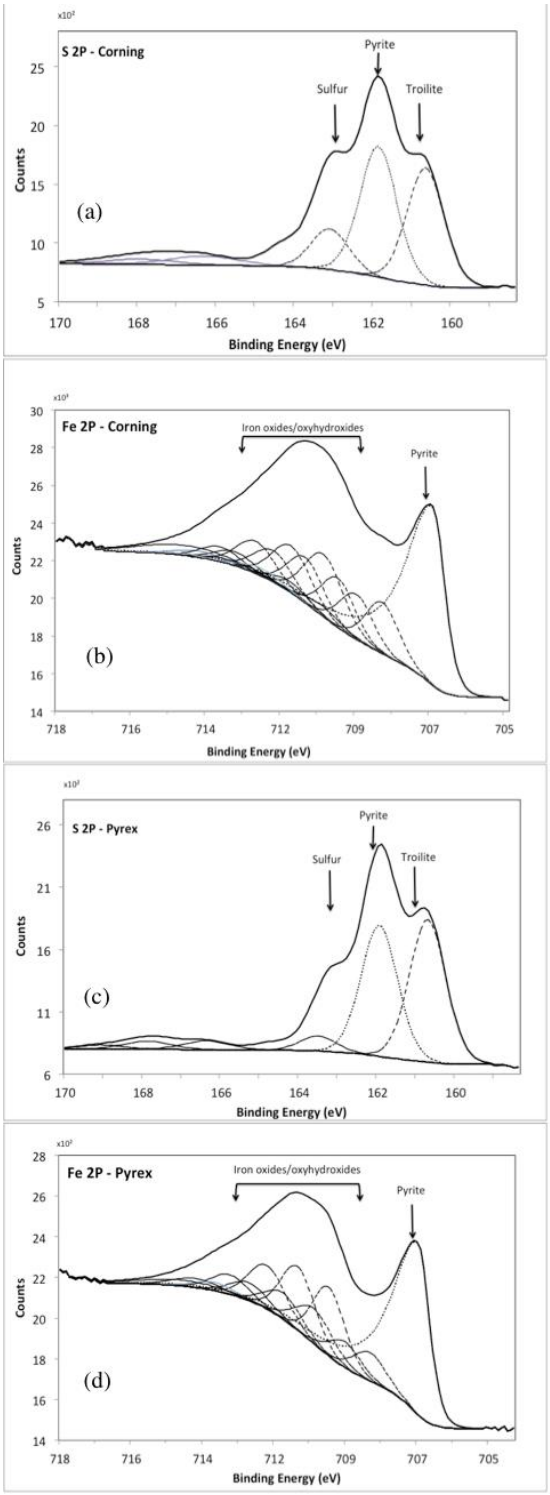

Fig. 4 S 2*p* (a,c) and Fe 2*p* (b,d) XPS of the films on corning (a,b) and pyrex (c,d) at 250℃

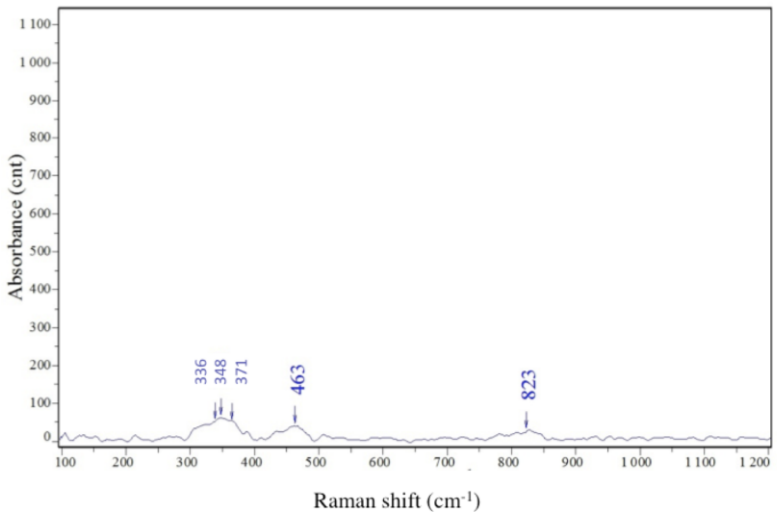

Fig. 5 Raman signal of thin film deposited on corning at 250˚C

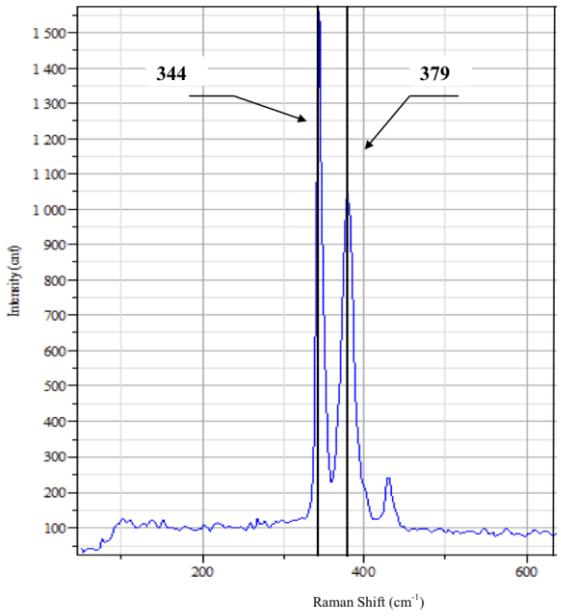

Fig. 6 Raman signal of natural iron pyrite

3.2 Natural target

XRD analysis of the natural target has shown that the latter consists of mainly iron pyrite. In contrast, the deposited films seem to consist primarily of pyrrhotite and sulphur, as revealed via XRD and shown in Fig. 8a, from room temperature up to 300℃. As the temperature is further increased, the films are made up of pyrrhotite, iron sulphide hydrate, and troilite as depicted in Fig. 8b.

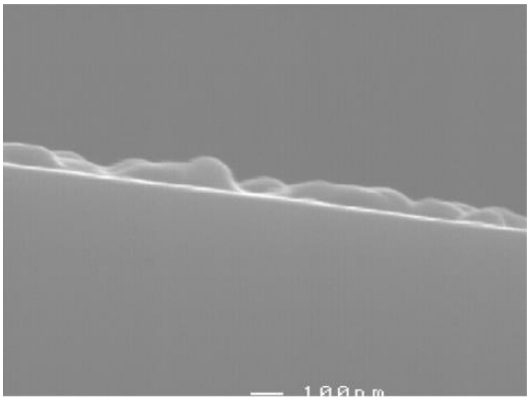

Fig. 7 Cross-section morphology of the film deposited on corning at 250℃

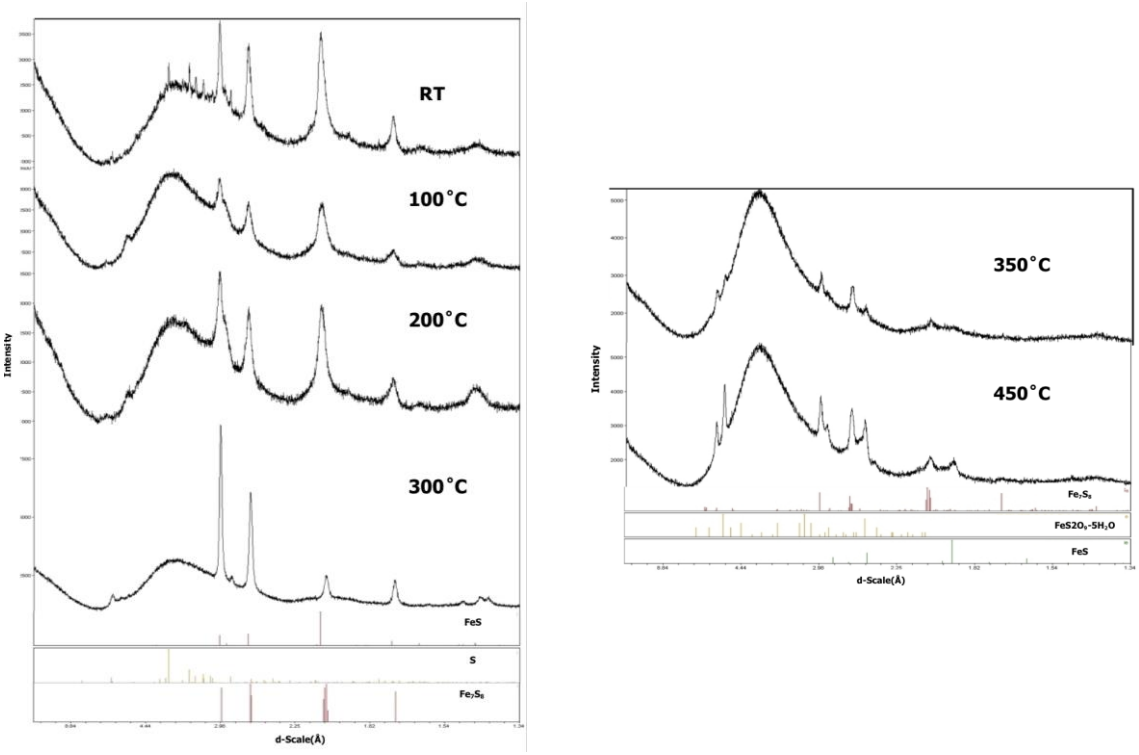

(a) (b)

Fig. 8 XRD difractogram of films deposited from the natural iron pyrite target: (a) RT-300℃ , (b) 350-450℃

5. Conclusions

Thin films consisting of iron pyrite have been deposited via pulsed electron ablation in an argon atmosphere from a single synthetic target made up of a mixture of elemental iron and sulfur. Various analysis techniques have revealed the presence of pyrite in the films at high substrate

temperature, namely, above 200℃. The films exhibit a rugged surface with nano-sized particulates. Films deposited from a natural pyrite target have not shown any evidence of pyrite in the temperature range RT-450℃. It is worthwhile to further investigate the effect of temperature on pyrite content of the thin films deposited from a synthetic target.

Acknowledgments

R. H. is grateful for financial support from the Natural Sciences and Engineering Research Council of Canada (NSERC).

References

Bronolda, M., Kubalaa, S., Pettenkofera, C. and Jaegermann, W. (1997), "Thin pyrite (FeS2) films by molecular beam deposition", *Thin Solid Films*, **304**, 178-182.

Chatzitheodorou, G., Fiechter, S., Konenkamp, R., Kunst, M., Jaegermann, W. and Tributsch, H. (1986), "Thin photoactive FeS_2 (pyrite) films", *Mater. Res. Bull*., **21**, 1481-1487.

Ennaoui, A. and Tributsch, H. (1984), "Iron sulphide solar cells", *Solar Cells*, **13**,197-200.

Jaegermann, W. and Tributsch, H. (1983), "Photoelectrochemical reactions of FeS_2 (pyrite) with H_2O and reducing agents", *J. Appl. Electrochemistry*, **13**, 743-750.

Kim, K. (1998), "Defect-associated photoluminescence and rapid thermal annealing effect on SiO_2 films grown in the plasma phase", *J. Vacuum Sci. Technol. A*, **16**, 2272-2276.

Lupis, C.H.P. (1983), *Chemical Thermodynamics of Materials*, North-Holland, Amsterdam, The Netherlands.

Nakamura, S. and Yamamoto, A. (2001), "Electrodeposition of pyrite (FeS_2) thin films for photovoltaic cells", *Solar Energy Materials and Solar Cells*, **65**, 79-85.

Parker, G.K. and Hope, G.A. (2010), "A Raman spectroscopic investigation of pyrite oxidation and flotation reagent interaction", *ECS Trans.*, **28**, 39-50.

Rezig, B., Dahman, H. and Kenzari, M (1992), "Iron pyrite FeS_2 for flexible solar cells", *Renewable Energy*, **2**, 125-128.

Sasaki, K. (1997), "Raman study of microbially-mediated solution of pyrite by thiobacillus ferroxidans", *The Canadian Mineralogist*, **35**, 999-1008.

Slater, J.C. (1965), *Quantum Theory of Molecules and Solids*, Vol. 2, McGraw-Hill, New York, USA.

Schlegel, A. and Wachter, P. (1976), "Optical properties, phonons and electronic structure of iron pyrite (FeS)", *J. Phys. C*, **9**, 3363-3396.

Seehra, S.S., Montano, P.A., Seehra, M.S. and Sen, S.K. (1979), "Preparation and characterization of thin films of FeS_2", *J. Materials Science*, **14**, 2761-2763.

Shembel, E.M., Polischuk, Y.V., Chervakov, O.V. and Reisner, D. (2006), "Reactivity of natural and synthesized FeS_2 relative to the components of polymer electrolytes", *Ionics*, **12**, 41-46.

van der Heide, H., Hemmel, R., van Bruggen, C.F. and Haas, C. (1980), "X-ray photoelectron spectra of 3d transition metal pyrites", *J. Solid State Chemistry*, **33**, 17-25.

Wadia, C., Alivisatos, A.P. and Kammen, D.M. (2009), "Materials availability expands the opportunity for large-scale photovoltaics deployment", *Environ. Sci. Technol.*, **43**, 2072-2077.

Wagner, C.D., Riggs, W.M., Davis, L.E., Moulder, J.F. and Mullenberg, G.E. (1979), *Handbook of X-ray Photoelectron Spectroscopy*, (Ed. Muilenberg, G.E.), Perkin-Elmer, Eden Prairie, MN, USA.

Willeke, G., Dasbach, R., Sailer, B. and Bucher, E. (1992), "Thin pyrite (FeS_2) films prepared by magnetron sputtering", *Thin Solid Films*, **213**, 271-276.

Yokoyama, D., Namiki, K. and Yamada, Y. (2006), "Mössbauer study of Fe/S and Fe/O films produced by

laser ablation of pyrite and hematite", *J. Radioanalytical and Nuclear Chemistry*, **268**, 283-288.

YH